

Construction of binary metal–organic cage–based materials via a “covalently linked plus cage encapsulated” strategy

Pei Lai†, Liang-Hua Wu, Lai-Yi Li, Song-Liang Cai, Sheng-Run Zheng*

GDMPA Key Laboratory for Process Control and Quality Evaluation of Chiral Pharmaceuticals, and Guangzhou Key Laboratory of Analytical Chemistry for Biomedicine, School of Chemistry, South China Normal University, Guangzhou 510006, China

* Corresponding author: Prof. Sheng-Run

E-mail address: zhengsr@scnu.edu.cn

Tel./Fax. : +86-20-39310187

Supporting Information

EXPERIMENTAL SECTION

Materials and Measurements

3,5-Di-pyridin-4-yl-benzaldehyde was of analytical grade and was obtained from Shanghai Kylpharm Co., Ltd. Other organic ligands were purchased from Shanghai Aladdin Biochemical Technology Co., Ltd. The other chemicals were of analytical grade and were purchased from Guangzhou Chemical Reagent Factory. Fourier transform infrared (FTIR) spectra (Platinum Elmer Spectrum) were measured with the KBr pressed-disc method in the range of 4000 to 400 cm^{-1} . Powder X-ray diffraction (PXRD) data were collected using Cu $K\alpha$ radiation ($k = 1.5406 \text{ \AA}$) at 40 kV and 40 mA at room temperature on an Ultima IV X-ray powder diffractometer. X-ray photoelectron spectroscopy (XPS) data were recorded on a Shimadzu AXIS SUPRA X-ray photoelectron spectrometer. Inductively coupled plasma (ICP) data were obtained on a Pastor Spectro Arcos MV Plasma Emission Spectrometer. SEM images were recorded on a German

ZEISS Ultra 55 field emission scanning electron microscope.

Synthesis of Pd–MOC

Pd-MOC was synthesized according to the literature.^{S1} A mixture of 3,5-di-pyridin-4-yl-benzaldehyde (52 mg, 0.20 mmol), Pd(NO₃)₂·2H₂O (26.6 mg, 0.10 mmol) and DMSO (6.0 mL) was added to a 15 mL high-pressure reaction bottle reactor. The air in the reactor was briefly replaced with argon and ultrasonicated for 10 min. The mixture was heated at 70 °C for 8 h to produce an orange yellow solution. The obtained solution was added to 24 mL of dioxane, and a white precipitate was obtained immediately. The white powder was separated by centrifugation and adequately washed with 24 mL of diethyl ether three times. Then, the white powder product was collected and dried under vacuum. Yield: 82% (based on Pd).

Synthesis of Al-MOC

Al-MOC was synthesized according to the literature.^{S2} AlCl₃·6H₂O (310 mg, 1.3 mmol) and 2,5-pyridinedicarboxylic acid (220 mg, 1.3 mmol) were dissolved in 10 mL of DMF by sonication for five minutes. Then, acetic acid (3.75 mL) was added. The solution was heated at 120 °C for 24 hours and then cooled to room temperature. After 3 days of storage, a white precipitate was formed and obtained through vacuum filtration. The solid was washed with fresh DMF, DMAc and acetone and then soaked overnight in fresh acetone. The precipitate was obtained by centrifugation and dried at 60 °C under vacuum to obtain the product. Yield: 70% (based on Al).

Synthesis of Ga–MOC

Ga-MOC was synthesized according to the literature.^{S3} A mixture of 4,5-imidazolium dicarboxylic acid (78 mg, 0.5 mmol), Ga(NO₃)₃·H₂O (128 mg, 0.5 mmol), and DMF (10 mL) was placed into a Teflon-lined stainless-steel autoclave. The mixture was heated at 120 °C for 24 hours and cooled to room temperature at 3 °C h⁻¹. The white powers of Ga–MOC were filtered. Yield 80% (based on Ga).

Synthesis of Fe–MOC

Ga-MOC was synthesized according to the literature.^{S4} 4,4-Diaminobenzene-2,2-disulfonic acid (0.834 g), pyridine-2-formaldehyde (0.5 mL), and sodium hydroxide (0.1932 g) were added to the flask. Then, 30 ml of deionized water that had been deoxidized for 20 minutes was added to the mixture and deoxidized for another 30 minutes. Then, 0.456 g of ferrous sulfate heptahydrate was added, and the mixture was further deoxygenated for 30 minutes. The solution was stirred at 50 °C for 18 hours

under argon gas. Half of the solvent was evaporated at 50-60 °C, and then 45 mL of acetonitrile was added with stirring. The resulting purple powder of Fe-MOC was obtained. Yield: 87% (based on Fe).

Synthesis of Cu-MOC

The synthesis of Cu-MOC was based on the method described in the literature.^{S5} First, 200 mg of copper acetate was dissolved in a mixed solvent of DMAc and methanol ($v_{\text{methanol}}: v_{\text{DMAc}} = 1:1$, 15 mL). Then, 5-sulfoisophthalic acid sodium salt (269 mg) methanol solution (8 mL) was added to the above solution. Then, 5 mL of DMAc and 40 μL of nitric acid were added, and the resulting solution was incubated for one week to obtain blue crystals of Cu-MOC. Yield: 63%.

Synthesis of Pd-MOC-TA

A mixture of Pd-MOC (90 mg, 0.01 mmol) and 5''-(4'-amino-[1,1'-biphenyl]-4-yl)-[1,1':4',1'':3'',1''':4''',1''''-quinque-phenyl]-4,4''''-diamine (TA, 46 mg, 0.08 mmol) was mixed evenly and then ground for 1 hour. The color of the mixture changed from pale gray to yellow. The mixture was washed with hot dimethyl sulfoxide (4 \times 15 mL), water (4 \times 15 mL) and acetone (3 \times 15 mL) to remove unreacted aMOC-1 and TA. Then, the mixture was heated at 100 °C for 24 h with a yield of 87% (based on Pd).

Synthesis of BMM-1

The synthesis method of BMM-1 is similar to that of Pd-MOC-TA, except that 67 mg of Al-MOC is added and ground together. Yield: 79% (based on Pd).

Synthesis of BMM-2

The synthesis method of BMM-1 is similar to that of Pd-MOC-TA, except that 60 mg of Ga-MOC is added and ground together. Yield: 79% (based on Pd).

Synthesis of BMM-1

The synthesis method of BMM-1 is similar to that of Pd-MOC-TA, except that 206 mg of Fe-MOC is added and ground together. Yield: 79% (based on Pd).

Synthesis of BMM-1

The synthesis method of BMM-1 was similar to that of Pd-MOC-TA, except that 52 mg of Cu-MOC was added and ground together, and the product was washed with dimethyl sulfoxide (4 \times 15 mL), methanol (4 \times 15 mL) and acetone (3 \times 15 mL). Yield: 79% (based on Pd).

Methanol adsorption by a quartz crystal microbalance (QCM)

AT-cut quartz crystals (gold-coated, 6 MHz resonant frequency) were employed

throughout the experiments. They were installed in a homemade gas phase pulse-measuring QCM system (Fig. S30), which contains a test chamber (500 mL), an oscillator detector, a temperature-control device, a frequency counter, and a computer. The QCM system was conditioned under nitrogen flow (400 mL/min) at a testing temperature before the measurement to obtain a stable frequency. The nitrogen gas was then turned off for a while and the frequency was recorded. Methanol (1 mL) was injected into the test chamber using a microsyringe. The corresponding frequency was recorded when the adsorption equilibrium of the QCM system was reached. The mass change of adsorption (Δm) is proportional to the frequency shift (Δf) in the electrode surface of the QCM. The equation is:

$$\Delta f = \frac{2f_0^2}{A\sqrt{\mu\rho}}\Delta m = -c\Delta m$$

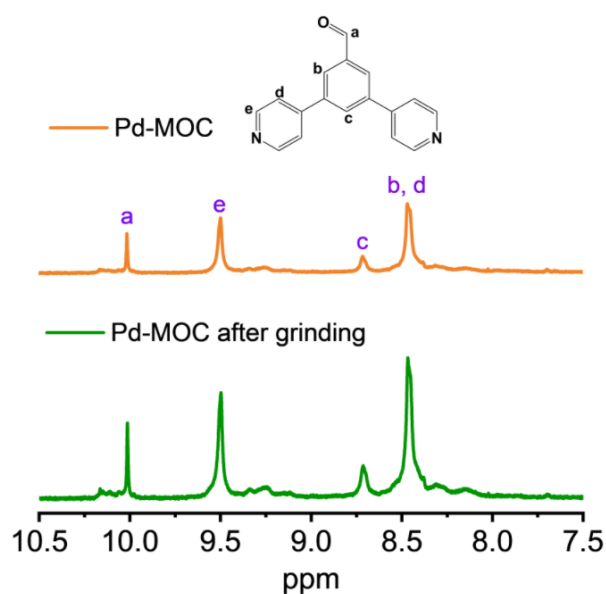


Fig. S1 ¹H NMR of Pd-MOC before and after grinding in DMSO-d₆.

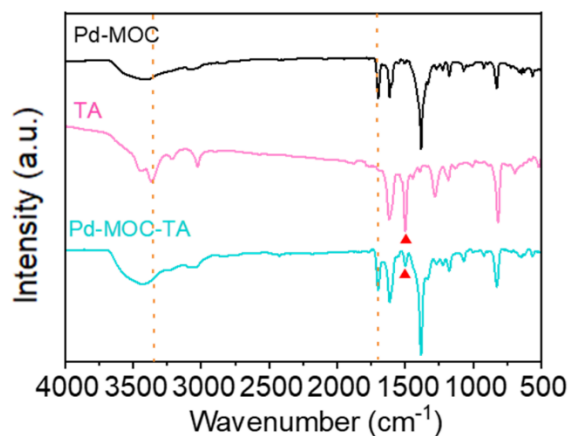


Fig. S2 FT-IR spectra of Pd-MOC, TA and Pd-MOC-TA.

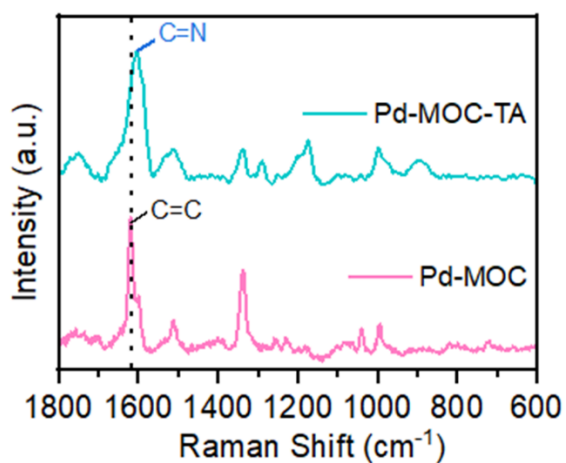


Fig. S3 Raman spectra of Pd-MOC and Pd-MOC-TA.

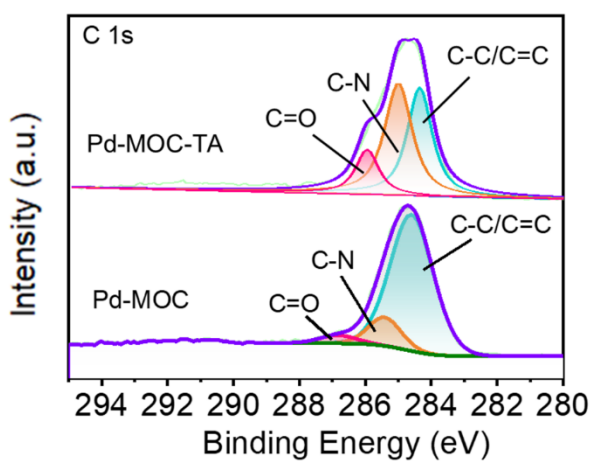


Fig. S4 High-resolution C 1s spectra of Pd-MOC and Pd-MOC-TA.

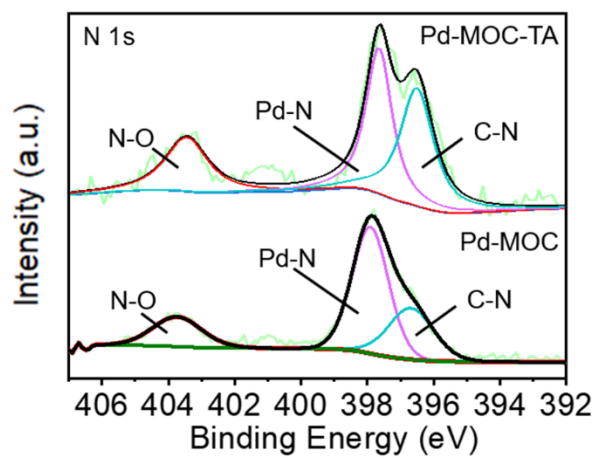


Fig. S5 High-resolution N 1s spectra of Pd-MOC and Pd-MOC-TA.

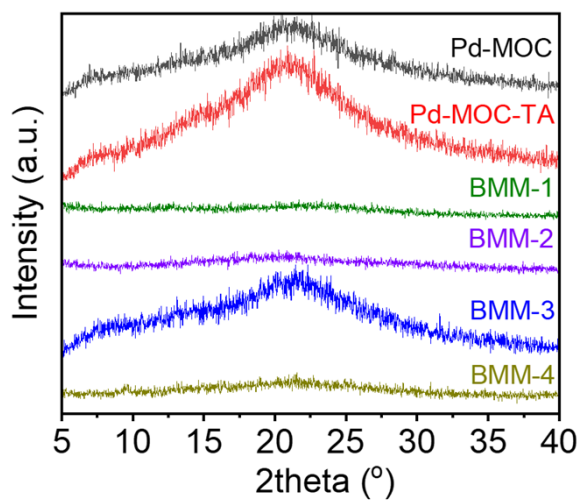


Fig. S6 PXRD patterns of Pd-MOC, Pd-MOC-TA, BMM-1, BMM-2, BMM-3, and BMM-4.

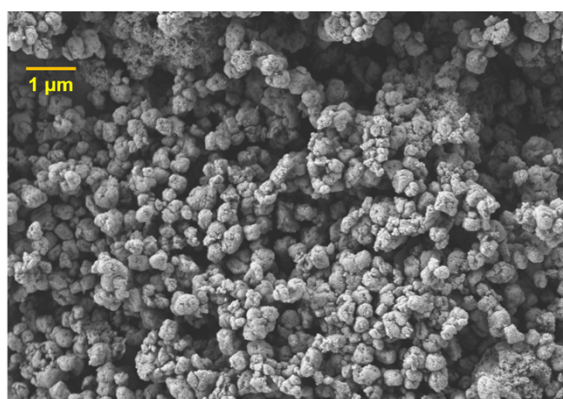


Fig. S7 The SEM of Pd-MOC-TA.

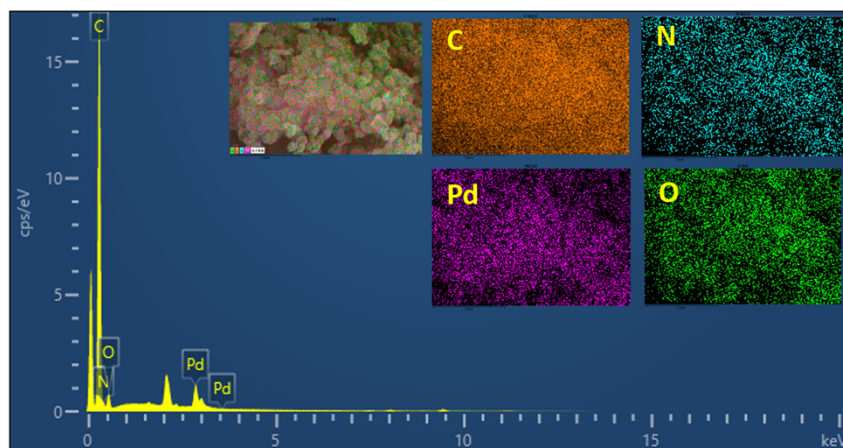


Fig. S8 The EDS of Pd-MOC-TA.

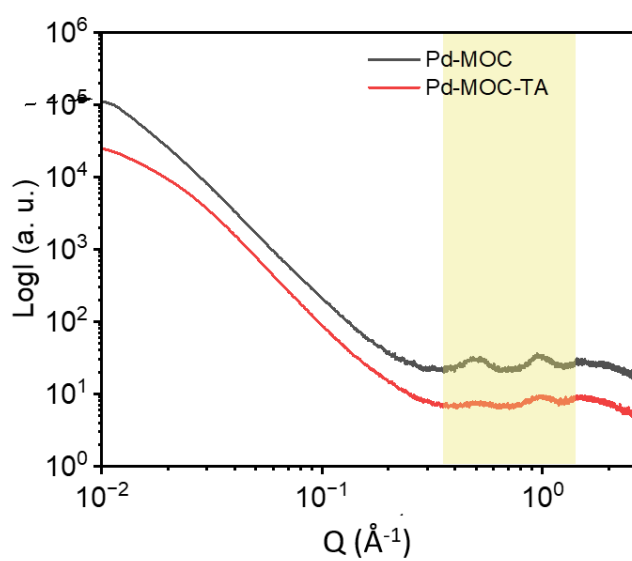


Fig. S9 SAXS profiles of Pd-MOC and Pd-MOC-TA.

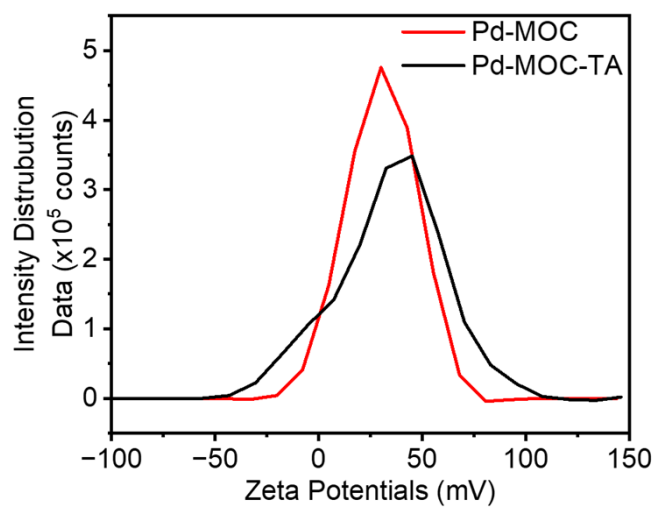


Fig. S10 The zeta potentials of Pd-MOC and Pd-MOC-TA.

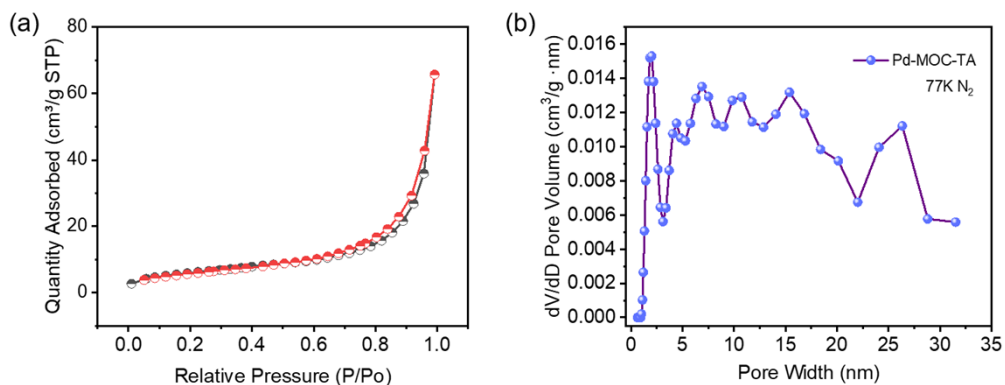


Fig. S11 (a) N₂ adsorption-desorption isotherms at 77 K and (b) pore size distribution of Pd-MOC-TA.

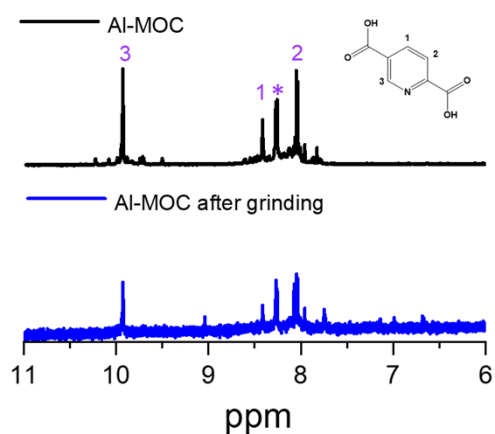


Fig. S12 ¹H NMR of Al-MOC before and after grinding in DMSO-d₆.

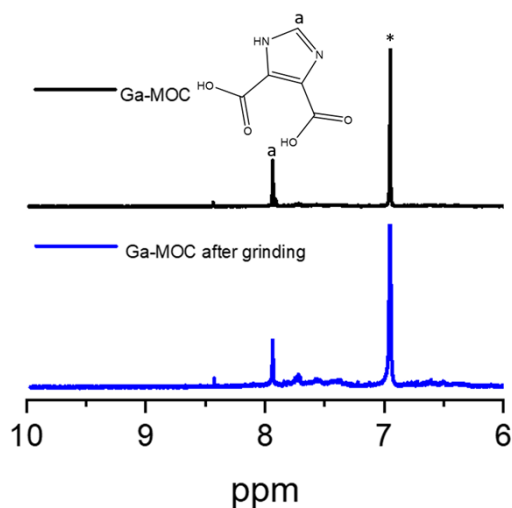


Fig. S13 ¹H NMR of Ga-MOC before and after grinding in DMSO-d₆.

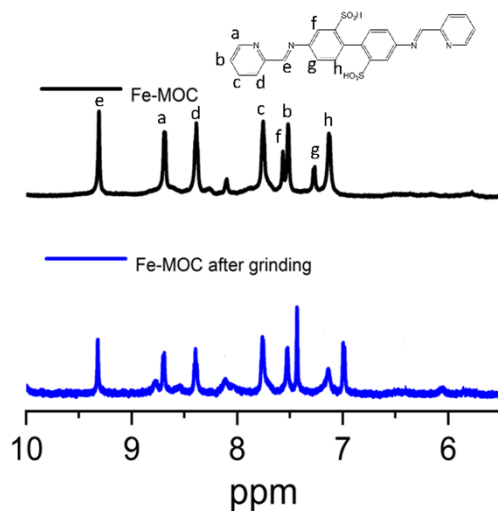


Fig. S14 $^1\text{H NMR}$ of Fe-MOC before and after grinding in DMSO-d_6 .

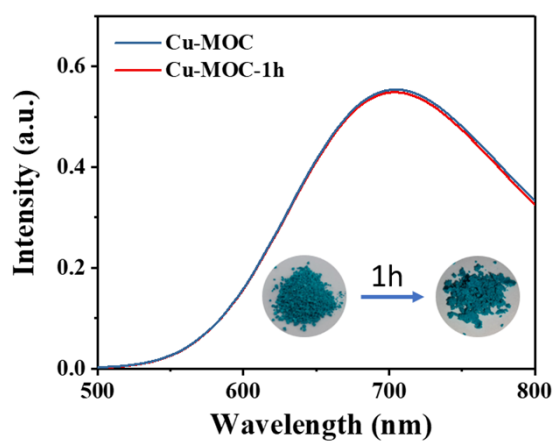


Fig. S15 UV-Vis spectra of Cu-MOC before and after grinding.

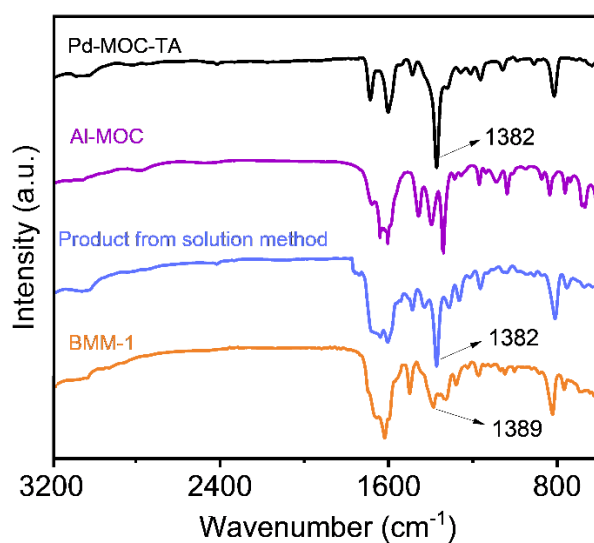


Fig. S16 Comparisons of IR spectra of Pd-MOC-TA, Al-MOC, BMM-1, and product from immersing Pd-MOC-TA in Al-MOC solution.

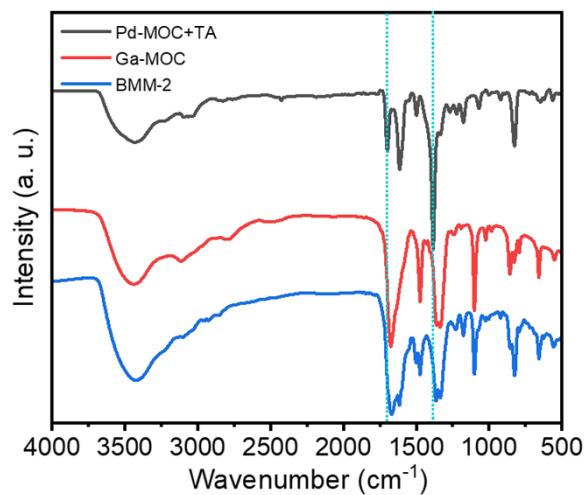


Fig. S17 The IR spectrum of BMM-2.

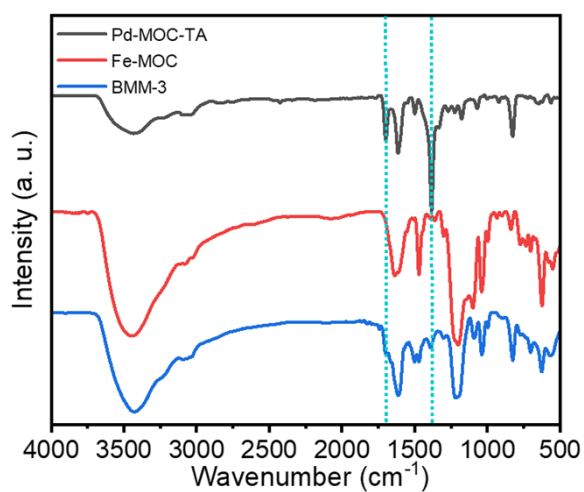


Fig. S18 The IR spectrum of BMM-3.

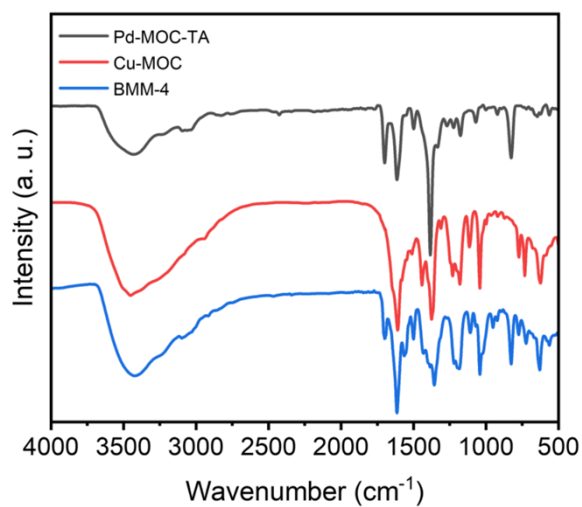


Fig. S19 The IR spectrum of BMM-4.

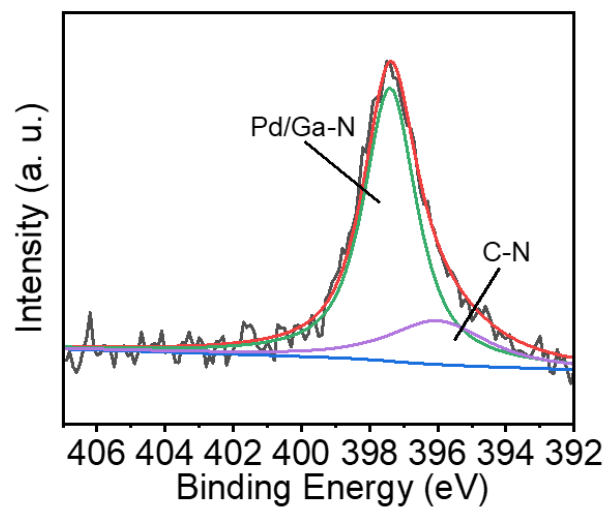


Fig. S20 The N 1s XPS spectrum of BMM-2.

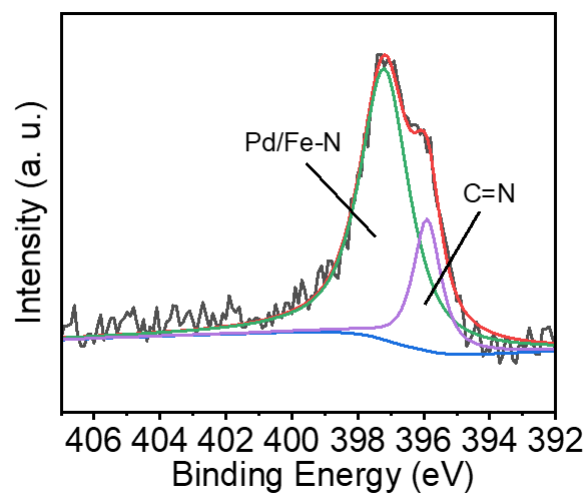


Fig. S21 The N 1s XPS spectrum of BMM-3.

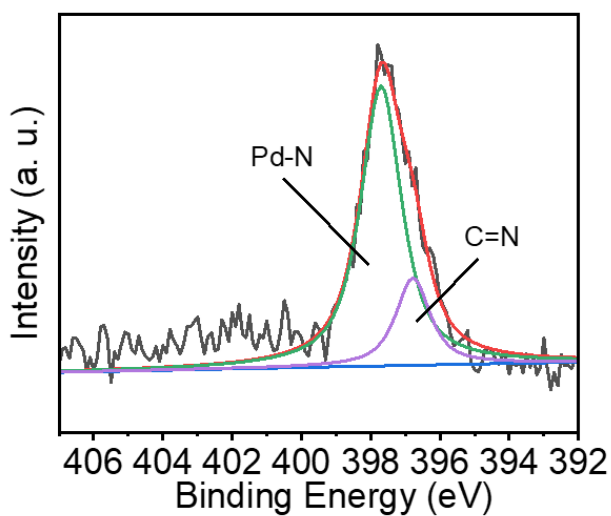


Fig. S22 The N 1s XPS spectrum of BMM-4.

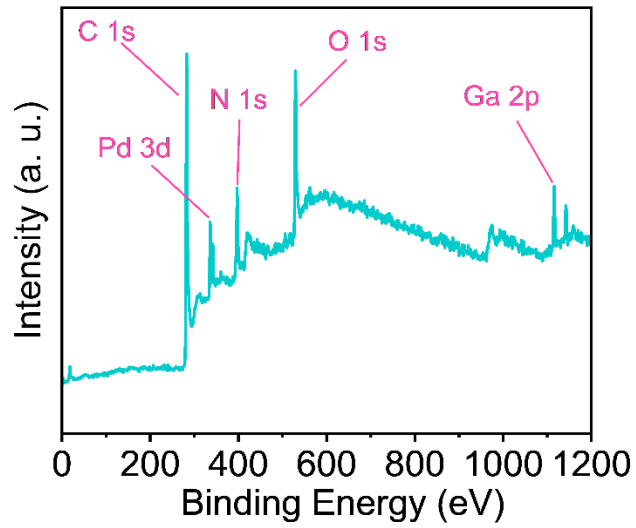


Fig. S23 XPS full spectrum of BMM-2.

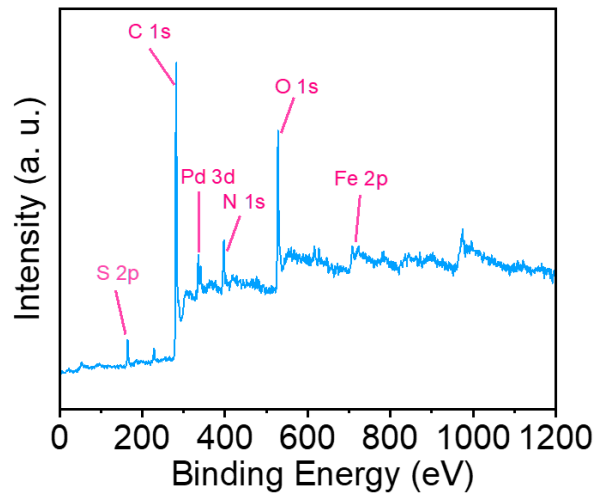


Fig. S24 XPS full spectrum of BMM-3.

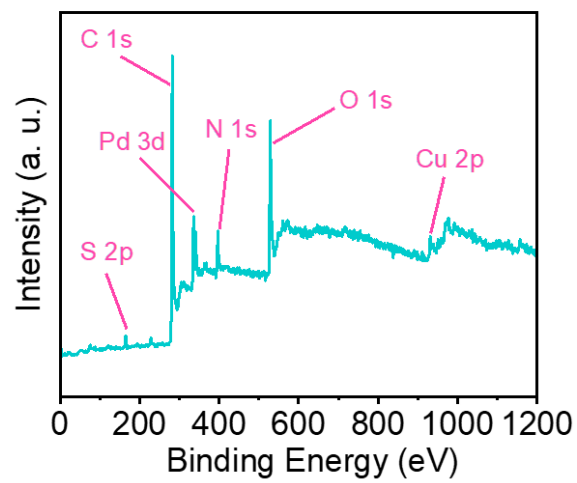


Fig. S25 XPS full spectrum of BMM-4.

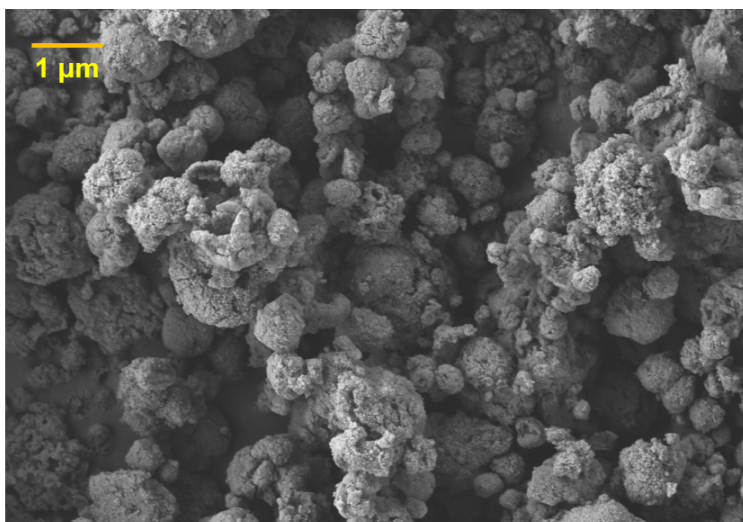


Fig. S26 SEM image of BMM-1.

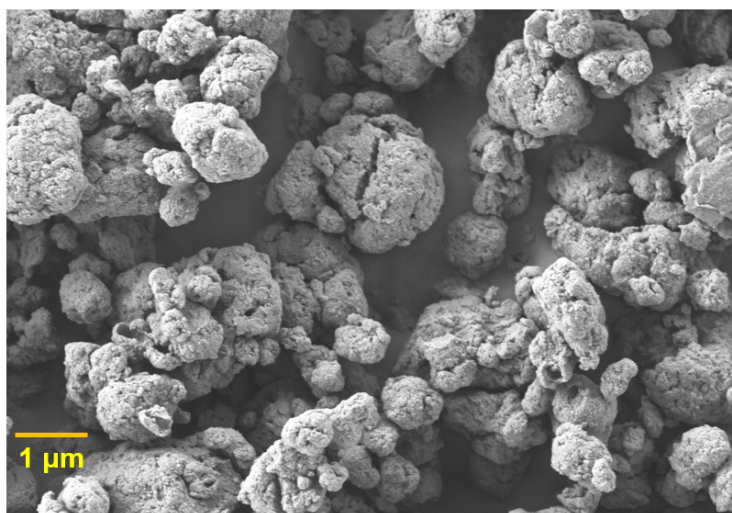


Fig. S27 SEM image of BMM-2.

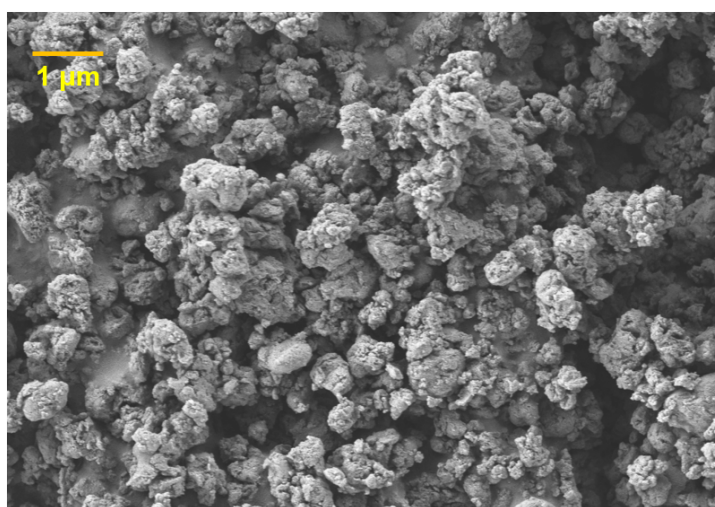


Fig. S28 SEM image of BMM-3.

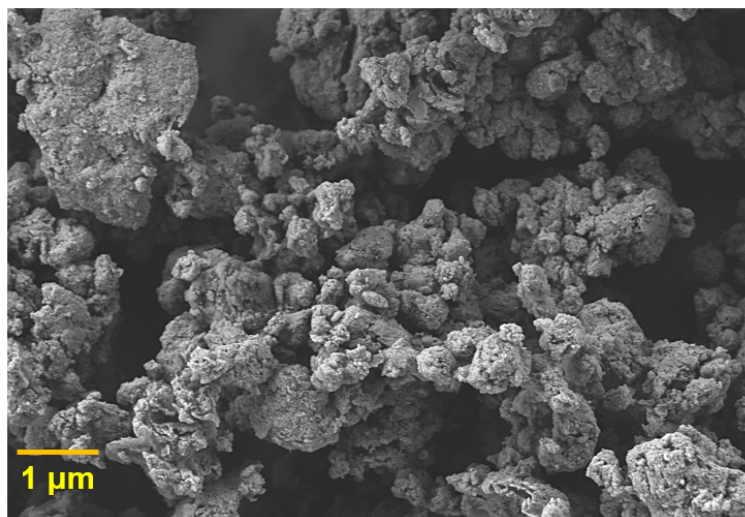


Fig. S29 SEM image of BMM-4.

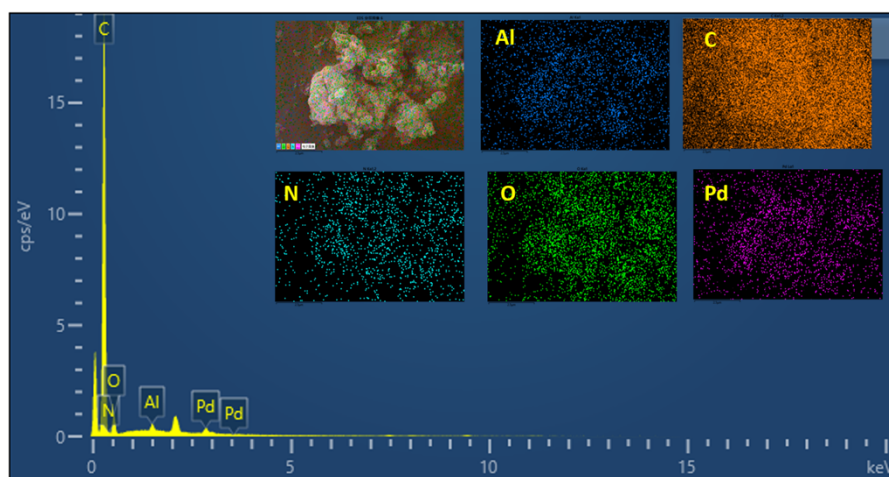


Fig. S30 EDS spectrum of BMM-1.

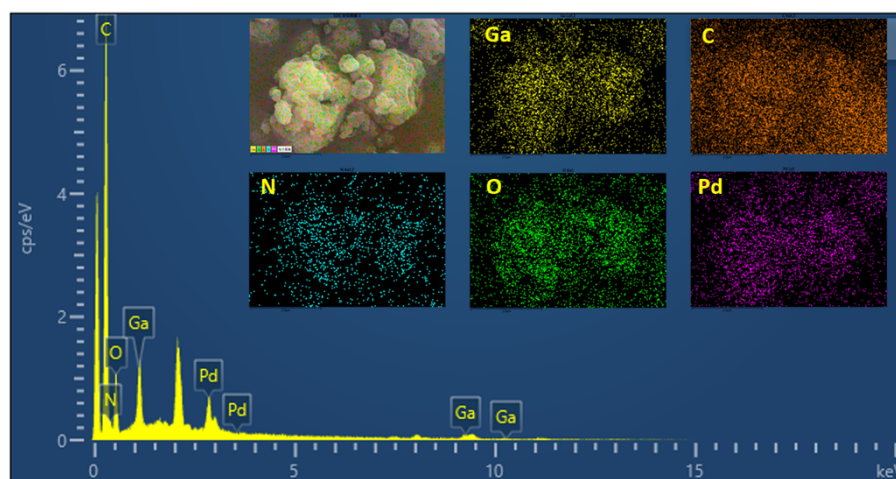


Fig. S31 EDS spectrum of BMM-2.

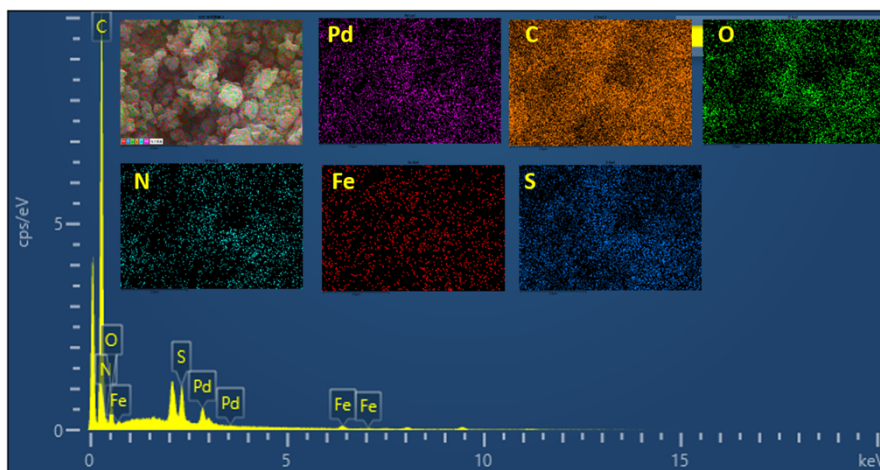


Fig. S32 EDS spectrum of BMM-3.

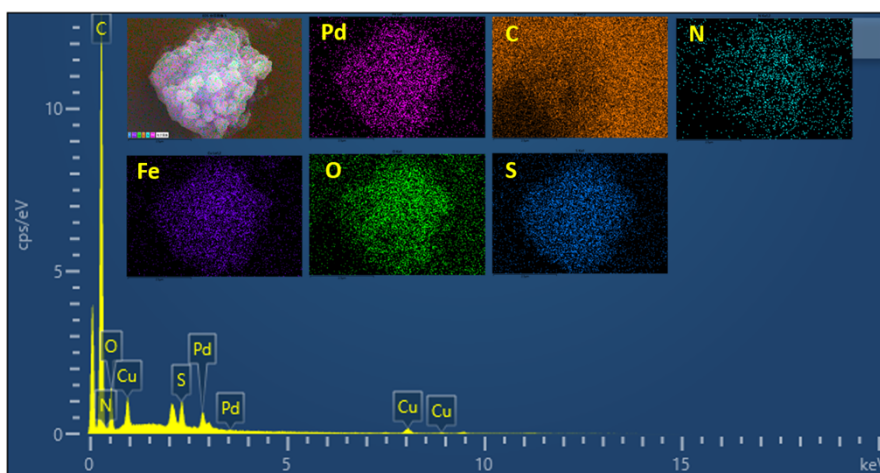


Fig. S33 EDS spectrum of BMM-4.

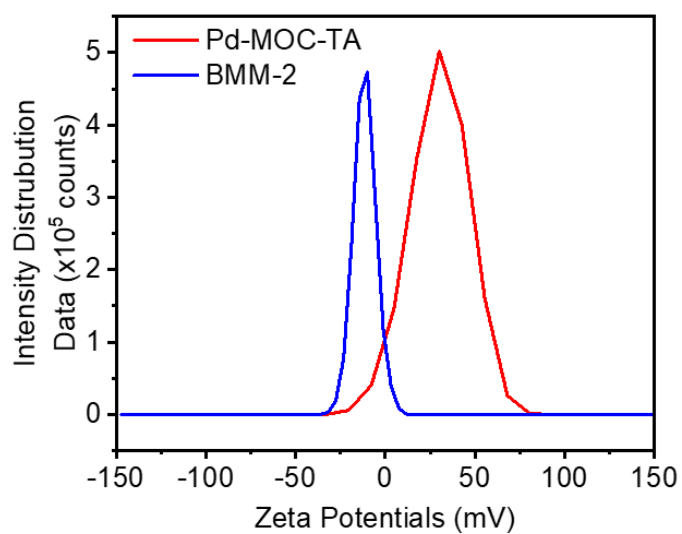


Fig. S34 The ζ -Potential of Pd-MOC-TA and BMM-2.

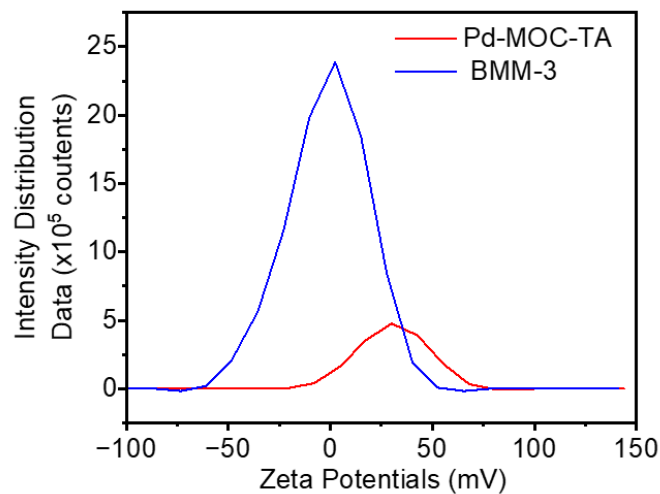


Fig. S35 The ζ -Potential of Pd-MOC-TA and BMM-3.

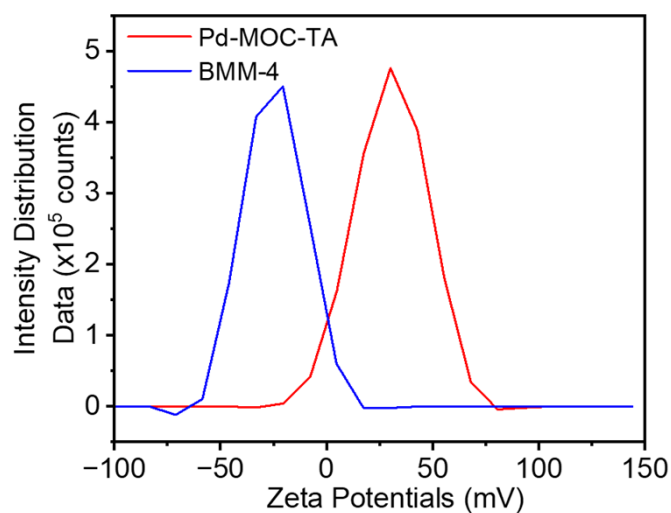


Fig. S36 The ζ -Potential of Pd-MOC-TA and BMM-4.

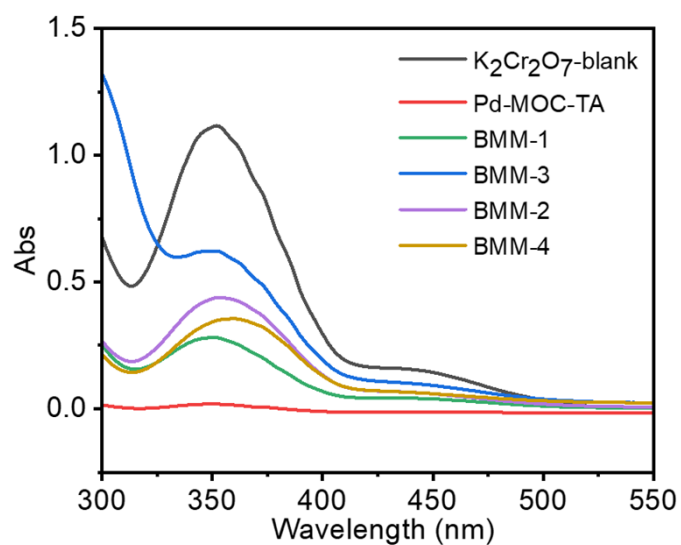


Fig. S37 The UV-Vis spectra of $\text{K}_2\text{Cr}_2\text{O}_7^{2-}$ before and after adding BMMs.

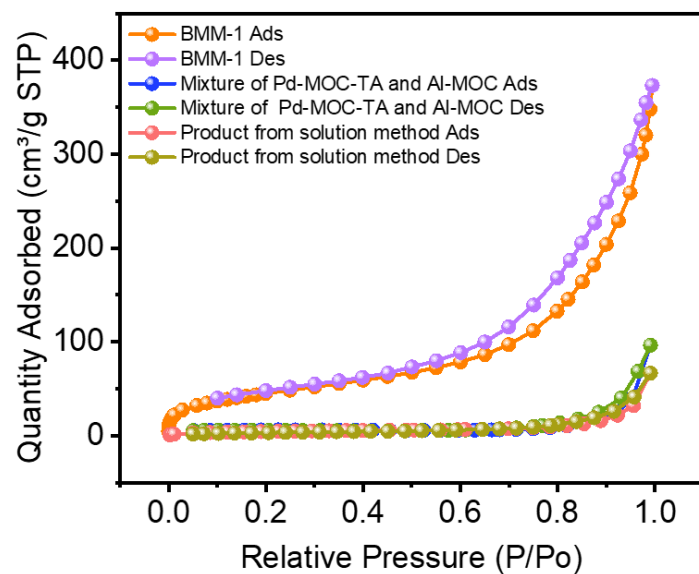


Fig. S38 Comparisons of N_2 adsorption-desorption isotherms at 77 K of BMM-1, mixture of Pd-MOC-TA and Al-MOC, and product form immersing Pd-MOC-TA in Al-MOC solution (solution method).

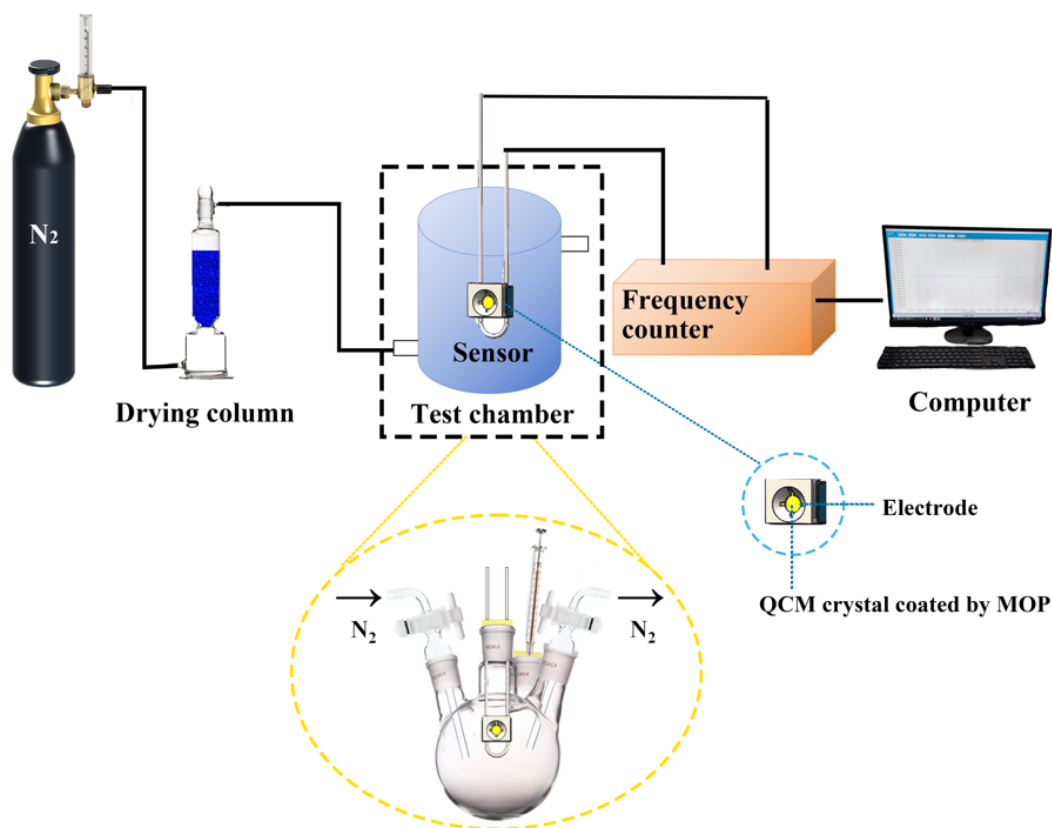


Fig. S39 The QCM setup.

Table S1. Comparisons of the ratio of metal ions from anionic MOC to Pd(II) for the ICP results and calculated results.

Samples	ICP results	Calculated
BMM-1	3.5:1	3:1
BMM-2	2.3:1	2:1
BMM-3	1:1.06	1:1
BMM-4	1:1.10	1:1

References

- S1. S.-Q. Deng, D.-M. Li, X.-J. Mo, Y.-L. Miao, S.-L. Cai, J. Fan, W.-G. Zhang, and S.-R. Zheng, *ChemPlusChem*, 2021, **86**, 709–715.
- S2. S. Ilic, A. M. May, P. M. Usov, H. D. Cornell, B. Gibbons, P. Celis-Salazar, D. R. Cairnie, J. Alatis, C. Slebodnick and A. J. Morris, *Inorg. Chem.*, 2022, **61**, 6604–6611.
- S3. P. Sutar, V. M. Suresh, K. Jayaramulu, A. Hazra and T. K. Maji, *Nat. Commun.*, 2018, **9**, 3587.
- S4. P. Mal, D. Schultz, K. Beyeh, K. Rissanen and J. R. Nitschke, *Angew. Chem. Int. Ed.*, 2008, **47**, 8297–8301.
- S5. J.-R. Li and H.-C. Zhou, *Nat. Chem.*, 2010, **2**, 893-898.